

**\*Highlights (for review)**

Highlights

- Hybrid solar cells using P3HT as donor and ZnO nanorods as acceptor were fabricated
- Benzoic acid based molecules were used for surface modification of ZnO as SAMs
- Linear relationship between dipole moment of SAMs and  $V_{oc}$  of devices was found
- Aggregation of the molecules was found in aqueous solution
- Ordered orientation of SAMs have better charge collecting properties

1  
2  
3  
4  
5  
6  
7  
8  
9  
10  
11  
12  
13  
14  
15  
16  
17  
18  
19  
20  
21  
22  
23  
24  
25  
26  
27  
28  
29  
30  
31  
32  
33  
34  
35  
36  
37  
38  
39  
40  
41  
42  
43  
44  
45  
46  
47  
48  
49  
50  
51  
52  
53  
54  
55  
56  
57  
58  
59  
60  
61  
62  
63  
64  
65

# Water-processed Self-assembles of Monolayers as Interface Modifier for ZnO/P3HT Hybrid Solar Cells

*Pipat Ruankham,<sup>1</sup> Susumu Yoshikawa<sup>2</sup> and Takashi Sagawa<sup>1\*</sup>*

<sup>1</sup>Graduate School of Energy Science, Kyoto University, Yoshida-Honmachi, Sakyo-Ku,  
Kyoto 606-8501, Japan

<sup>2</sup>Institute of Advanced Energy, Kyoto University, Gokasho, Uji, Kyoto, 611-0011, Japan

E-mail address: [patto@iae.kyoto-u.ac.jp](mailto:patto@iae.kyoto-u.ac.jp) (P. Ruankham) , [s-yoshi@iae.kyoto-u.ac.jp](mailto:s-yoshi@iae.kyoto-u.ac.jp) (S.Yoshikawa)  
, [sagawa.takashi.6n@kyoto-u.ac.jp](mailto:sagawa.takashi.6n@kyoto-u.ac.jp) (T.Sagawa)

Corresponding author at: Graduate School of Energy Science, Kyoto University, Yoshida-Honmachi,  
Sakyo-Ku, Kyoto 606-8501, Japan Tel: +81-75-753-5624. Fax: +81-75-753-5627.

E-mail address: [sagawa.takashi.6n@kyoto-u.ac.jp](mailto:sagawa.takashi.6n@kyoto-u.ac.jp) (T.Sagawa)

1  
2  
3 **Abstract**  
4

5 Benzoic acid based molecules were used for surface modification of ZnO nanorods as self-assembled  
6 monolayers (SAMs) in order to improve the interface interaction between ZnO and poly(3-  
7 hexylthiophene) in hybrid solar cells. The dipole moment of the molecules and the solvent used for the  
8 surface modification were investigated in relation to the performance of the hybrid devices. A linear  
9 relationship between the dipole moment of the interface modifiers and the open circuit voltage ( $V_{oc}$ ) of  
10 the devices were found. The  $V_{oc}$  are enhanced by the use of the molecules with their dipole moment  
11 pointing away from the ZnO surface and vice versa. The enhancement in  $V_{oc}$  is attributed to the shift of  
12 the vacuum level of ZnO when the surface is modified by the SAMs. When water was used as the  
13 solvent for surface modification process, aggregate was found in the solution state. This implies an  
14 ordered orientation of SAMs attached onto the ZnO surface, resulting in the improvement of the  $V_{oc}$ .  
15 An enhancement in the incident photon to current efficiency spectra was also obtained in the devices  
16 prepared from aqueous solution. The SAMs prepared from aqueous solution have better charge  
17 collecting properties in comparison to that prepared from ethanol solution.  
18  
19  
20  
21  
22  
23  
24  
25  
26  
27  
28  
29  
30  
31  
32  
33  
34  
35  
36  
37  
38

39 **Keywords**  
40

41 Interface modification, ZnO nanorod, SAM, solvent, hybrid solar cell  
42  
43  
44  
45  
46  
47  
48  
49  
50  
51  
52  
53  
54  
55  
56  
57  
58  
59  
60  
61  
62  
63  
64  
65

## 1. Introduction

In recent years, hybrid inorganic/polymer photovoltaic devices (HPVs) have been broadly studied because of their fundamental research interest and application potential. The concept of HPVs is a combination of organic materials (p-type polymers) and inorganic ones (n-type nanostructured metal oxides) [1, 2]. Many inorganic materials such as  $\text{TiO}_2$ [3],  $\text{ZnO}$ [2, 4],  $\text{Si}$ [5, 6] and so on, have been selected as an electron acceptor in HPVs. Among these inorganic materials, vertically-aligned  $\text{ZnO}$  nanorods show good potential for an application in HPVs and other electronic devices because of their low temperature processability [7, 8] and high carrier mobilities with a direct electron pathway to the electrode [9, 10].

However, when an HPV is fabricated by pairing the most widely used p-type donor, poly(3-hexylthiophene) (P3HT) with the  $\text{ZnO}$  nanorods, measured power conversion efficiencies (PCEs) are quite low in comparison to conventional organic photovoltaic devices (OPVs) [11, 12]. In our previous report [2], we reported an approach to improve the photovoltaic performance of HPV by surface modification with organic dye molecules with different functional group and absorption range. It was found clearly that the improvement in short circuit current density ( $J_{sc}$ ) corresponds to the extension of the absorption range of the devices when squaraine dyes, which absorb light in the near infrared region, are used. Moreover, open circuit voltage ( $V_{oc}$ ) of the devices shows a relationship with the dipole moment ( $\mu$ ) of the interface modifier. The enhanced  $V_{oc}$  can be achieved by attaching the dye molecules with their  $\mu$  pointing away from the  $\text{TiO}_2$  surface [13, 14], and the same effect could be expected for  $\text{ZnO}$ .

However, the selected dyes have different functional group and molecular size, which may affect the  $V_{oc}$  and fill factor ( $FF$ ) of the devices [15]. In this work, self-assemble monolayers (SAMs) are used as the interface modifier for the  $\text{ZnO}$  nanorods since their dipole moment can change the surface potential of the adsorbing surface [16, 17]. Benzoic acid based molecules with different *para* groups

1  
2  
3 are selected because they provide a range of different magnitudes and direction of the  $\mu$ . Moreover, the  
4  
5 effects of the solvent for SAMs modification are investigated to study the adsorption mechanism on  
6  
7 ZnO and the relationship to the photovoltaic performances.  
8  
9

## 10 11 12 2. Experimental section 13 14

15 The ZnO nanorods were synthesized by the method described in previously reported procedures  
16  
17 [2]. Dense ZnO layers, serving as seed for the ZnO nanorods, were prepared by spin coating a 1:1  
18  
19 molar mixture of Zn acetate and monoethanolamine in 2-methoxyethanol on ITO substrates. After that,  
20  
21 the substrates were annealed on a hot plate at 300°C for 10 min. The hydrothermal growth of ZnO  
22  
23 nanorod arrays was carried out by suspending the seed substrates in an aqueous solution of zinc nitrate  
24  
25 hexahydrate and hexamethylenetetramine at 90°C. The resulting length of the nanorods is  
26  
27 approximately 240 nm. Then, the substrates were carefully rinsed with distilled water and annealed at  
28  
29 150°C for 10 min.  
30  
31  
32  
33

34 Surface modification with benzoic acid based SAMs was performed by immersing the ZnO  
35  
36 nanorods substrates in solutions (30  $\mu$ M) of benzoic acid (BA), 4-aminobenzoic acid (ABA), 4-  
37  
38 (diethylamino)benzoic acid (DBA), 4-nitrobenzoic acid (NBA), and 4-cyanobenzoic acid (CBA) in  
39  
40 ethanol or deionized water at room temperature for 1 h. The substrates were carefully rinsed with  
41  
42 ethanol or deionized water after the deposition of SAMs.  
43  
44  
45

46 A solution of P3HT in chlorobenzene (30 mg ml<sup>-1</sup>) was spin-coated on top of the SAMs-  
47  
48 modified ZnO nanorods and subsequently annealed at 150°C for 3 min in a N<sub>2</sub> filled glove box. Finally,  
49  
50 the MoO<sub>x</sub> (15 nm) and Ag top electrode (100 nm) was thermally deposited in a vacuum evaporation  
51  
52 system. The basic schematic structure of the devices is shown in Figure 1.  
53  
54  
55

56 The dipole moment calculation was performed by using single-point electronic structure with  
57  
58 semi-empirical MOPAC program with PM3 model in HyperChem package. UV-vis absorption  
59  
60  
61

1  
2  
3 measurement was carried out using a UV-Vis spectrophotometer (UV-2450 Shimadzu). The  
4  
5 photocurrent-voltage characteristics were characterized under ambient atmosphere and simulated solar  
6  
7 light, AM 1.5, 100 mW cm<sup>-2</sup> (CEP-2000 Bunkoh-Keiki). The light intensity was calibrated by using a  
8  
9 standard silicon photodiode (BS520, Bunkoh-Keiki).  
10

### 11 12 13 14 15 3. Results and discussion 16

17 The morphologies of the ZnO nanorods prepared by hydrothermal growth are shown in Figure  
18  
19 2a. The diameter and length are about 25 nm and 240 nm, respectively. The P3HT is able to infiltrate  
20  
21 into rod-to-rod space as confirmed by the cross-sectional FE-SEM images in Figure 2b. For the device  
22  
23 with surface modification, there is no expected change in the morphologies of ZnO nanorods after  
24  
25 immersing the as-prepared ZnO nanorod substrates into the ethanol and aqueous solutions, since the  
26  
27 concentration of the solution is low (30 μM), yielding pH values of about 7. Also, the p*K*<sub>a</sub> values of the  
28  
29 SAMs are in the range of 3.4-4.6, which indicate that the solutions of SAMs are weak acid.  
30  
31  
32

33  
34 In order to find the effect of dipole moment on the photovoltaic performance, the  $\mu$  of the  
35  
36 benzoic acid based molecules were calculated using semi-empirical models from the HyperChem  
37  
38 software. The orientations of the molecules used for calculating  $\mu$  are in such a way that the *C2* axis of  
39  
40 the carboxylate is parallel to the *z*-axis, while the ZnO surface plane is parallel to the *x*- and *y*-axes.  
41  
42 This is because interface molecules generally attach to metal oxide or metal surfaces by their  
43  
44 carboxylic or carboxylate group [18, 19]. After the adsorption of SAMs on the ZnO surface, the  
45  
46 magnitude of dipole moment may change since the carboxylic group lessens in its electron-  
47  
48 withdrawing property. However this change is not significant [14]. The evaluated magnitudes and  
49  
50 directions of  $\mu$  are shown in Table 1 and Figure 3a. It can be seen that the  $\mu$  of BA, ABA, and DBA  
51  
52 points away from the ZnO surface while one of CBA and NBA points toward the ZnO surface. Note  
53  
54 that the positive value of  $\mu$  indicates its direction pointing away from the ZnO surface.  
55  
56  
57  
58  
59  
60  
61

1  
2  
3 Figure 3b and 3c compares the optimized molecular structure and electron distribution of  
4 benzoic acid based molecules at highest occupied molecular orbital (HOMO) and lowest unoccupied  
5 molecular orbital (LUMO). The electron density is distributed over the benzene rings and *para* group  
6 of the molecules at the HOMO state, while the electron distribution over the carboxylic group of the  
7 molecules is also observed at the LUMO state. This indicates that under illumination, the photoexcited  
8 electron is directed to inject into the conduction band of the ZnO via carboxylic group of the molecules.  
9 This confirms that the molecules are able to act as the interface modifier of a semiconductor.

10  
11  
12 The molecules were attached onto the ZnO surface by using either water or ethanol as the  
13 solvent. The photovoltaic performances of the devices corresponding to the change in  $\mu$  of the SAMs  
14 are plotted in Figure 4. The relation between  $J_{sc}$  of the hybrid devices and the  $\mu$  of the molecules is not  
15 clear as seen in Figure 4a. The  $J_{sc}$  is rather related to the light absorption range of the modifying  
16 molecules and the tail of the modifiers facing P3HT [2]. Moreover, the use of water as solvent for  
17 SAMs is found to yield higher  $J_{sc}$  than the use of ethanol. This is because SAMs prepared from an  
18 aqueous solution have higher level of ordering on the ZnO surface and less surface impurities than the  
19 ones prepared from ethanol solution. The role of electron transport will be explained below.

20  
21  
22 A linear relationship between the  $\mu$  of the molecules and  $V_{oc}$  (Figure 4b) was found. The  $V_{oc}$  of  
23 the devices modified with BA, ABA, and DBA is relatively high in comparison to that of the device  
24 modified with NBA and CBA. This is attributed to the  $\mu$  of BA, ABA, and DBA pointing away from  
25 the ZnO surface, resulting in the downward shift of the vacuum level of the ZnO semiconductor  
26 (passing from ZnO to P3HT) and greater band bending at the ZnO/P3HT interface [13, 14]. The highest  
27 improvement in  $V_{oc}$  of the devices is obtained from the device modified with ABA in aqueous solution.  
28 The  $V_{oc}$  of the ABA device increases from 0.39 V for the unmodified device to 0.41 V and 0.46 V for  
29 the devices using ethanol and water as solvent, respectively.

1  
2  
3 In Figure 4c, the plot between the  $\mu$  of SAMs and the fill factor ( $FF$ ) of the hybrid devices also  
4 shows a linear relationship, which is similar to the trend of  $\mu$  and  $V_{oc}$  (Figure 4b). However, the use of  
5 benzoic acid based molecules with the  $\mu$  pointing away from the ZnO surface does not show a  
6 significant improvement in  $FF$  in comparison to the unmodified devices. This indicates that the charge  
7 recombination at the ZnO/P3HT interface modified with small molecules is not significantly reduced in  
8 comparison to the case of the devices modified with large molecules such as C60-SAMs [1] and dye  
9 molecules [2], which have a longer charge carrier lifetime [15].  
10  
11  
12  
13  
14  
15  
16  
17  
18  
19  
20

21 It is seen clearly that the molecules with dipole moment pointing toward the ZnO surface  
22 deteriorate both  $V_{oc}$  and  $FF$  of the devices. However, for the molecule with dipole moment pointing  
23 away from the ZnO surface, the expected improvement in  $V_{oc}$  and  $FF$  from the calculated dipole  
24 moment of the SAMs could not be achieved since the actual dipole moment of the ZnO/SAMs complex  
25 is less than the dipole moment of the SAMs. This is because of the interfacial dipole between  $COO^-$   
26 group and ZnO that points toward ZnO [16]. The highest power conversion efficiency ( $PCE$ ) of 0.53%  
27 is achieved from the ABA-modified device prepared from aqueous solution (Figure 4d), while one  
28 prepared from ethanol solution shows lower  $PCE$  of 0.41%, which is mainly due to lower  $J_{sc}$  and  $V_{oc}$ .  
29  
30  
31  
32  
33  
34  
35  
36  
37  
38  
39

40 In order to understand the effect of solvent and the  $\mu$  of SAMs on the  $V_{oc}$  of the device, reverse  
41 saturation current density ( $J_0$ ) was extracted from  $JV$  curve (Figure 5a) under the dark conditions by  
42 using the diode equation [20];  
43  
44  
45  
46

$$47 \quad J = J_0 (e^{qV/nk_B T} - 1)$$

48 where  $J_0$  is reverse saturation current density,  $n$  is ideality factor,  $q$  is the elementary charge,  $k$  is  
49 Boltzmann constant and  $T$  is temperature. The equation can be fitted well to the dark  $JV$  curve in an  
50 exponential regime ( $0.1 < V < 0.4$ ) as shown in Figure 5b. The plot between the extracted  $J_0$  and the  $\mu$   
51 of the SAMs in Figure 6 represents a linear relationship. This is attributed to the leakage-blocking  
52 behavior of the electric field generated by the  $\mu$  with their direction pointing away from the surface [2].  
53  
54  
55  
56  
57  
58  
59  
60  
61  
62  
63  
64  
65



1  
2  
3 The reduction of  $J_0$  would increase the  $V_{oc}$  of the device which is described by the equation  $V_{oc} =$   
4  
5  $(nkT/q)\ln(J_{sc}/J_0+1)$ [2].  
6

7  
8 For the effect of solvent on the photovoltaic performances, the absorbance and  
9  
10 photoluminescence of ABA in ethanol and aqueous solution at various concentrations were measured  
11  
12 and the resulting spectra are shown in Figure 7. When the concentration of the solution increases, the  
13  
14 red shift, which was found only in the case of aqueous solution (Figure 7a), was observed. This  
15  
16 indicates that there is an aggregate formation of the molecules in the solution state. This maybe  
17  
18 attributed to a high polarity of water, which prefers to interact with a carboxylic group than the benzene  
19  
20 ring of the interface modifier molecules. Since an interaction among benzene rings of the benzoic based  
21  
22 molecules is not disturbed by the existence of water molecules, allowing the molecules to form the  
23  
24 aggregate. While, the shift of the absorbance peak and photoluminescence peak was not found in the  
25  
26 case of ethanol solution (Figure 7b). This is because a non-polar part of ethanol may interact with the  
27  
28 benzene ring of the SAM molecules, blocking the aggregate formation.  
29  
30  
31  
32  
33

34  
35 When the molecules are adsorbed onto the ZnO surface, the interaction among the molecules  
36  
37 may weaken due to the strong interaction between ZnO and their carboxylic group. On the other hand,  
38  
39 the orientation of SAMs prepared from aqueous solution may have a higher level of ordering on the  
40  
41 ZnO surface than one prepared from ethanol solution because of the aggregation in the solution state.  
42  
43 The deprotonated molecules of ethanol ( $CH_3CH_2O^-$ ) are able to coordinate to the Zn atoms, forming a  
44  
45 coordination bonding of Zn-OCH<sub>2</sub>CH<sub>3</sub> [21]. Coordinated  $CH_3CH_2O^-$  disrupts the orientation of SAMs  
46  
47 and serves as the interface impurity. Similarly, the molecules of water can also coordinate to the Zn  
48  
49 atoms, forming  $Zn(OH_2)_n$ , though the  $Zn(OH_2)_n$  is a native surface impurity of ZnO nanorods prepared  
50  
51 from hydrothermal method [4, 22].  
52  
53  
54  
55

56  
57 The orientation of SAMs and the presence of the surface impurity affect the charge generation  
58  
59 and charge harvesting properties of the devices as confirmed by an incident photon to current  
60  
61

1  
2  
3 efficiency (*IPCE*) measurement (Figure 8). In comparison to the unmodified device, the device  
4  
5 prepared from aqueous solution shows the enhancement in *IPCE* spectra in both UV and visible region,  
6  
7 which relate to the photo-generated charge carrier of ZnO and P3HT, respectively [2, 23]. However,  
8  
9 the device prepared from ethanol solution does not show the enhancement in *IPCE* spectra in the  
10  
11 visible region. This demonstrates that the SAMs-modified ZnO film prepared from aqueous solution  
12  
13 has better potential to accept electrons from P3HT than one prepared from ethanol solution. One of the  
14  
15 reasons is that electrons cannot transport through an alkane tail of the Zn-OCH<sub>2</sub>CH<sub>3</sub> complex.  
16  
17  
18  
19  
20  
21

#### 22 4. Conclusions

23  
24  
25 In conclusion, an approach for the improvement of photovoltaic performance of hybrid solar  
26  
27 cells based on ZnO nanorods and P3HT by modification of SAMs was presented. ABA-modified  
28  
29 device prepared from aqueous solution gave the best *PCE* of about 0.53%. The improved performance  
30  
31 of ABA-modified devices was mainly attributed to the dipole moment which points away from the  
32  
33 ZnO surface, resulting in the enhancement of  $V_{oc}$  and the reduction of  $J_0$ . The orientation of SAMs on  
34  
35 the ZnO surface, which is found in case of the use of water as solvent, shows the improvement in  $V_{oc}$   
36  
37 and  $J_{sc}$  in comparison to the SAMs-modified device prepared from ethanol solution. Ethanol is not the  
38  
39 proper solvent of SAMs because of the presence of Zn-OCH<sub>2</sub>CH<sub>3</sub> as the surface impurity.  
40  
41  
42  
43  
44  
45

#### 46 Acknowledgement

47  
48  
49 Authors gratefully acknowledged the New Energy and Industrial Technology Development  
50  
51 Organization (NEDO) of the Ministry of Economy, Trade, and Industry (METI), and Core Research of  
52  
53 Evolutional Science & Technology Agency (CREST) from Japan Science Technology Agency (JST) in  
54  
55 addition to Global Centers of Excellence (GCOE) Program from the Ministry of Education, Culture,  
56  
57 Sports, Science & Technology (MEXT).  
58  
59  
60  
61  
62  
63  
64  
65

1  
2  
3 Figure 1. Schematic device structure of ZnO nanorods/P3HT hybrid solar cell.  
4

5 Figure 2. FE-SEM images: a) top view of ZnO nanorods and b) cross-sectional view of the ZnO  
6  
7 nanorods/P3HT hybrid device.  
8  
9

10 Figure 3. a) Semi-empirical calculation of stabilized molecular structure and dipole moment (arrows)  
11  
12 of benzoic acid based molecules and their charge distribution of the b) HOMO and c) LUMO  
13  
14 orbitals.  
15  
16

17 Figure 4. Photovoltaic performance, a) short-circuit current density ( $J_{sc}$ ), b) open-circuit voltage ( $V_{oc}$ ),  
18  
19 c) fill factor ( $FF$ ), and d) power conversion efficiency ( $PCE$ ), of the ZnO nanorods/P3HT  
20  
21 hybrid solar cells with different SAMs in ethanol (red square) and water (blue circle).  
22  
23  
24

25 Figure 5. Photocurrent – voltage ( $J-V$ ) curves for the ZnO nanorods/P3HT hybrid devices without and  
26  
27 with surface modification of the ZnO with ABA in ethanol, ABA in water, NBA in ethanol,  
28  
29 and NBA in water under dark condition plotted on a semi-log scale in a range of a) -1.0 V to  
30  
31 2.0 V and b) 0 V to 0.5 V. The diode equation (solid line in b) is well fitted to experimental  
32  
33 data (open symbol).  
34  
35  
36

37 Figure 6. The extracted  $J_0$  of the ZnO nanorods/P3HT hybrid solar cells with different SAMs in  
38  
39 ethanol (red square) and water (blue circle) plotted versus the dipole moment of the SAMs.  
40  
41

42 Figure 7. Normalized absorbance (solid line) and photoluminescence spectra (dash line) of ABA  
43  
44 solution in water (a) and ethanol (b) at various concentrations (35  $\mu\text{M}$  – 250  $\mu\text{M}$ ).  
45  
46

47 Figure 8. Comparison of  $IPCE$  spectra of the devices with unmodified (black) and SAMs-modified  
48  
49 ZnO nanorods prepared fom ethanol (red) and water (blue) solution.  
50  
51  
52  
53  
54  
55  
56  
57  
58  
59  
60  
61  
62  
63  
64  
65

- 1  
2  
3 [1] S.K. Hau, Y.J. Cheng, H.L. Yip, Y. Zhang, H. Ma, A.K.Y. Jen, *Acs. Appl. Mater. Inter.* 2 (2010)  
4  
5 1892-1902.  
6  
7  
8 [2] P. Ruankham, L. Macaraig, T. Sagawa, H. Nakazumi, S. Yoshikawa, *J. Phys. Chem. C* 115 (2011)  
9  
10 23809-23816.  
11  
12 [3] Q.D. Tai, X.Z. Zhao, F. Yan, *J. Mater. Chem.* 20 (2010) 7366-7371.  
13  
14  
15 [4] P. Ruankham, T. Sagawa, H. Sakaguchi, S. Yoshikawa, *J. Mater. Chem.* 21 (2011) 9710-9715.  
16  
17 [5] C.Y. Liu, Z.C. Holman, U.R. Kortshagen, *Adv. Funct. Mater.* 20 (2010) 2157-2164.  
18  
19 [6] S. Jeong, E.C. Garnett, S. Wang, Z. Yu, S. Fan, M.L. Brongersma, M.D. McGehee, Y. Cui, *Nano*  
20  
21 *Lett.* 12 (2012) 2971-2976.  
22  
23  
24 [7] L. Vayssieres, *Adv. Mater.* 15 (2003) 464-466.  
25  
26 [8] L.E. Greene, M. Law, D.H. Tan, M. Montano, J. Goldberger, G. Somorjai, P.D. Yang, *Nano Lett.* 5  
27  
28 (2005) 1231-1236.  
29  
30  
31 [9] A.L. Briseno, T.W. Holcombe, A.I. Boukai, E.C. Garnett, S.W. Shelton, J.J.M. Frechet, P.D. Yang,  
32  
33 *Nano Lett.* 10 (2010) 334-340.  
34  
35  
36 [10] B.Q. Sun, E. Marx, N.C. Greenham, *Nano Lett.* 3 (2003) 961-963.  
37  
38  
39 [11] D.C. Olson, Y.J. Lee, M.S. White, N. Kopidakis, S.E. Shaheen, D.S. Ginley, J.A. Voigt, J.W.P.  
40  
41 Hsu, *J. Phys. Chem. C* 112 (2008) 9544-9547.  
42  
43  
44 [12] P. Atienzar, T. Ishwara, B.N. Illy, M.P. Ryan, B.C. O'Regan, J.R. Durrant, J. Nelson, *J. Phys.*  
45  
46 *Chem. Lett.* 1 (2010) 708-713.  
47  
48  
49 [13] J. Krüger, U. Bach, M. Grätzel, *Adv. Mater.* 12 (2000) 447-451.  
50  
51  
52 [14] C. Goh, S.R. Scully, M.D. McGehee, *J. Appl. Phys.* 101 (2007) 114503.  
53  
54 [15] M. Miyashita, K. Sunahara, T. Nishikawa, Y. Uemura, N. Koumura, K. Hara, A. Mori, T. Abe, E.  
55  
56 Suzuki, S. Mori, *J. Am. Chem. Soc.* 130 (2008) 17874-17881.  
57  
58  
59 [16] H.-L. Yip, S.K. Hau, N.S. Baek, H. Ma, A.K.Y. Jen, *Adv. Mater.* 20 (2008) 2376-2382.  
60  
61  
62  
63  
64  
65

1  
2  
3  
4  
5  
6  
7  
8  
9  
10  
11  
12  
13  
14  
15  
16  
17  
18  
19  
20  
21  
22  
23  
24  
25  
26  
27  
28  
29  
30  
31  
32  
33  
34  
35  
36  
37  
38  
39  
40  
41  
42  
43  
44  
45  
46  
47  
48  
49  
50  
51  
52  
53  
54  
55  
56  
57  
58  
59  
60  
61  
62  
63  
64  
65

[17] H.-L. Yip, S.K. Hau, N.S. Baek, A.K.Y. Jen, Appl. Phys. Lett. 92 (2008) 193313-193313.

[18] K.E. Lee, M.A. Gomez, S. Elouatik, G.P. Demopoulos, Langmuir, 26 (2010) 9575-9583.

[19] Y. Liang, B. Peng, J. Chen, J. Phys. Chem. 114 (2010) 10992-10998.

[20] G.A.H. Wetzelaer, M. Kuik, M. Lenes, P.W.M. Blom, Appl. Phys. Lett. 99 (2011).

[21] G. Kwak, K. Yong, J. Phys. Chem. 112 (2008) 3036-3041.

[22] Q. Ahsanulhaq, A. Umar, Y.B. Hahn, Nanotechnology 18 (2007) -.

[23] D.C. Olson, Y.J. Lee, M.S. White, N. Kopidakis, S.E. Shaheen, D.S. Ginley, J.A. Voigt, J.W.P. Hsu, J. Phys. Chem. C 111 (2007) 16640-16645.

Table 1. Dipole moment of benzoic acid based molecules.

SAMs	$\mu_x$	$\mu_y$	$\mu_z$	$ \mu _{\text{total}}$
BA	0	1.19	1.91	2.23
ABA	0	2.97	3.10	4.29
DBA	0.22	1.22	4.51	4.68
NBA	0	0.74	-3.62	-3.69
CBA	0	0.18	-2.05	-2.05

Figure 1

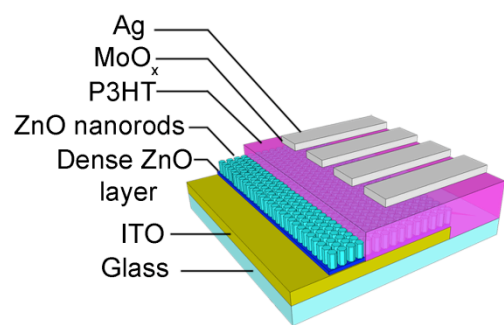


Fig 1

Figure 2

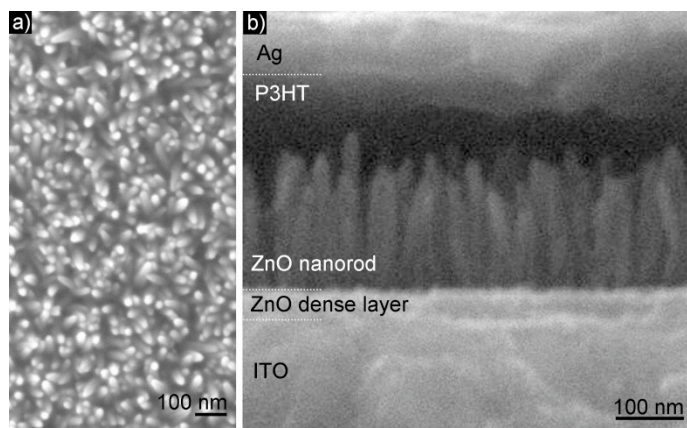


Fig 2



Figure 3

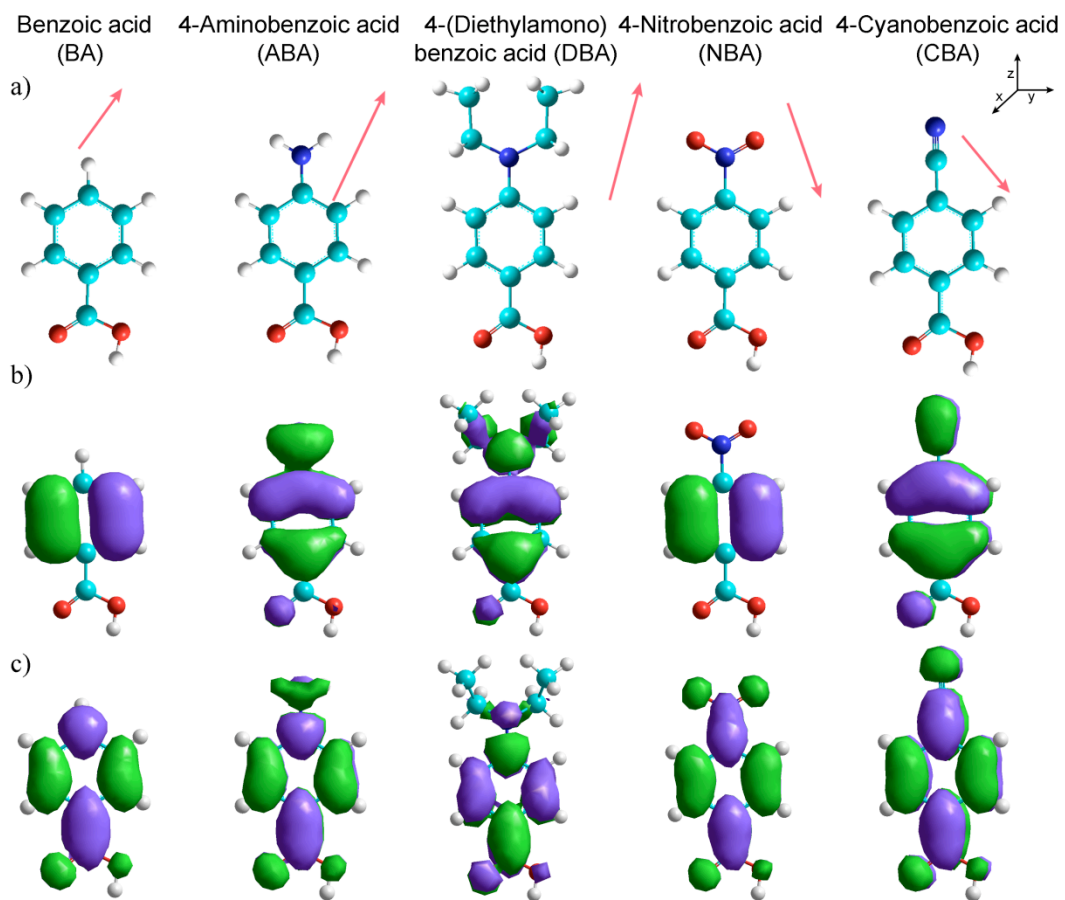


Fig 3

Figure 4

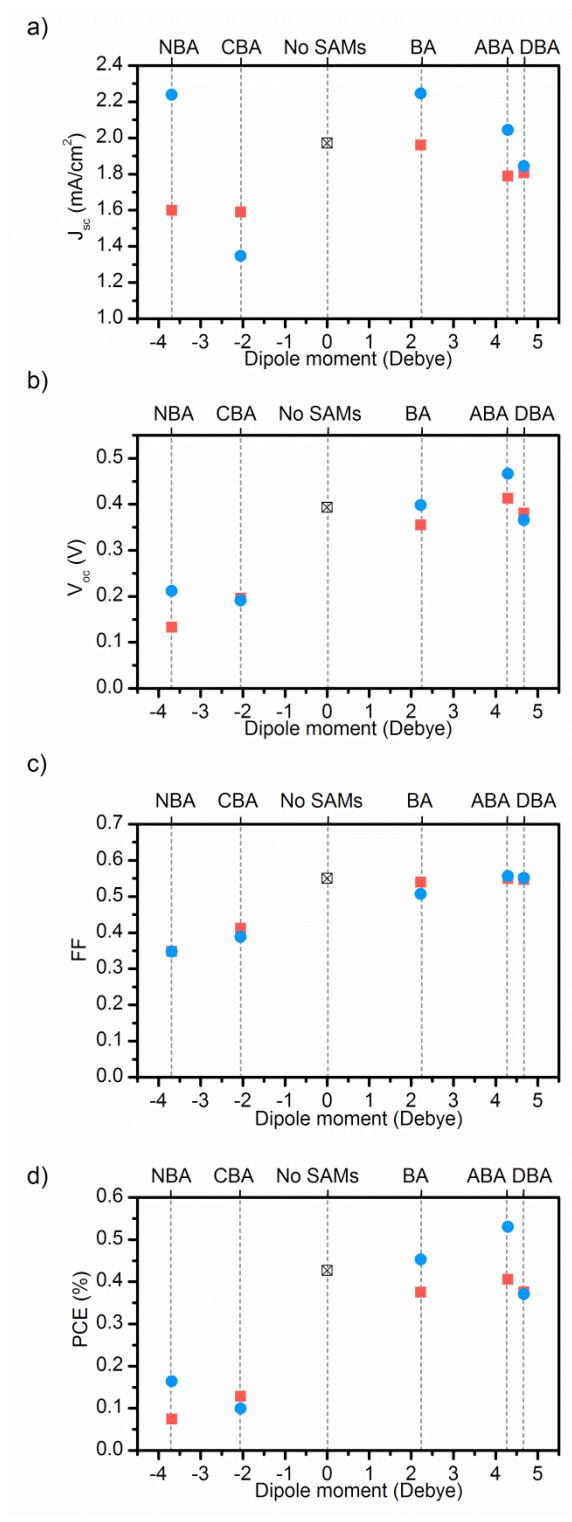


Fig 4

Figure 5

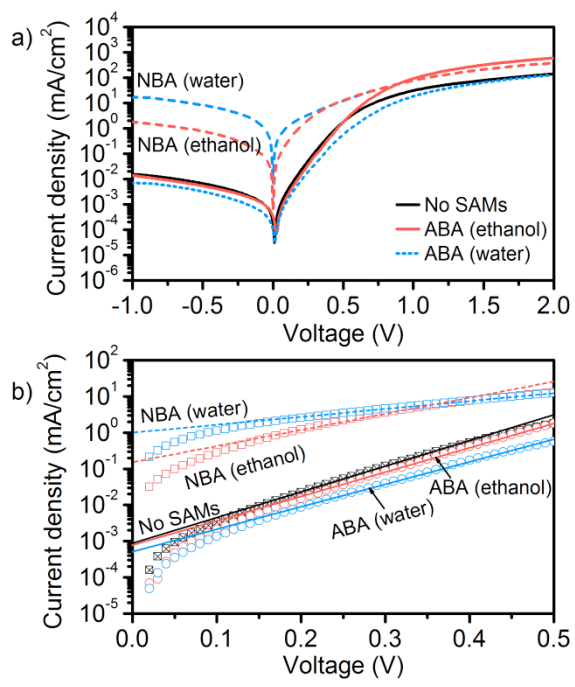


Fig 5

Figure 6

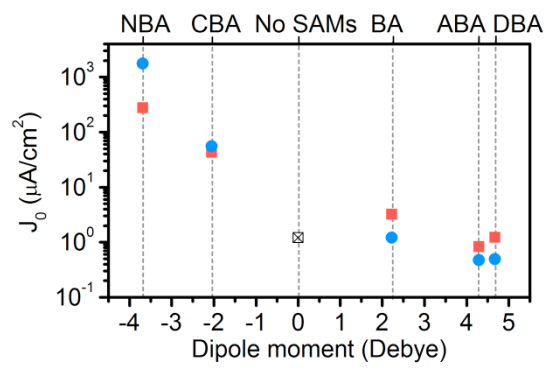


Fig 6

Figure 7

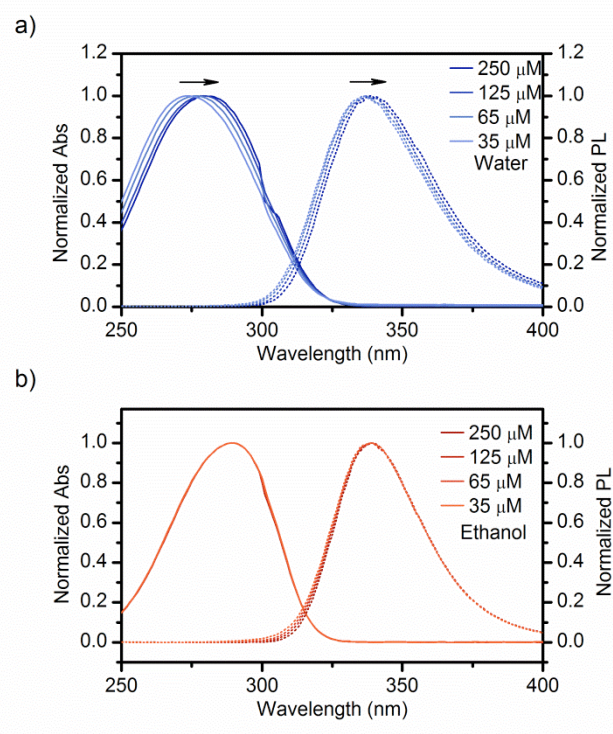


Fig 7

Figure 8

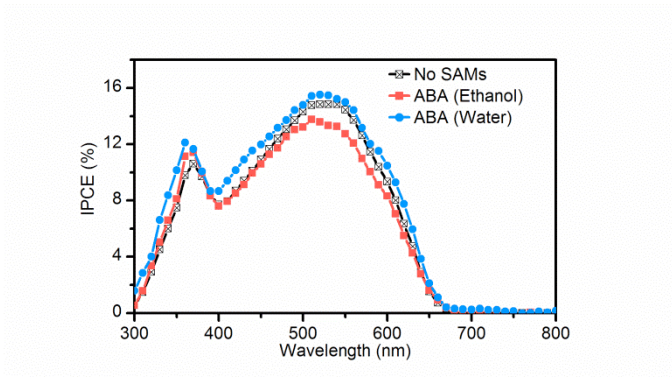


Fig 8